Materials Science and Engineering C 49 (2015) 34–39

Contents lists available at ScienceDirect

Materials Science and Engineering C

journal homepage: www.elsevier.com/locate/msec

Electrochemical deoxyribonucleic acid biosensor based on electrodeposited graphene and nickel oxide nanoparticle modified electrode for the detection of salmonella enteritidis gene sequence

Wei Sun [a,*], Xiuli Wang [b], Yongxi Lu [b], Shixing Gong [b], Xiaowei Qi [b], Bingxin Lei [a], Zhenfan Sun [a], Guangjiu Li [b,*]

[a] College of Chemistry and Chemical Engineering, Hainan Normal University, Haikou 571158, PR China
[b] College of Chemistry and Molecular Engineering, Qingdao University of Science and Technology, Qingdao 266042, PR China

ARTICLE INFO

Article history:
Received 6 October 2014
Received in revised form 7 December 2014
Accepted 17 December 2014
Available online 19 December 2014

Keywords:
Carbon ionic liquid electrode
Graphene
NiO nanoparticle
Electrodeposition
Electrochemical DNA biosensor

ABSTRACT

In this paper a new electrochemical DNA biosensor was prepared by using graphene (GR) and nickel oxide (NiO) nanocomposite modified carbon ionic liquid electrode (CILE) as the substrate electrode. GR and NiO nanoparticles were electrodeposited on the CILE surface step-by-step to get the nanocomposite. Due to the strong affinity of NiO with phosphate groups of ssDNA, oligonucleotide probe with a terminal 5′-phosphate group could be attached on the surface of NiO/GR/CILE, which could further hybridize with the target ssDNA sequence. Methylene blue (MB) was used as the electrochemical indicator for monitoring the hybridization reaction. Under the optimal conditions the reduction peak current of MB was proportional to the concentration of salmonella enteritidis gene sequence in the range from 1.0×10^{-13} to 1.0×10^{-6} mol L^{-1} with a detection limit as 3.12×10^{-14} mol L^{-1}. This electrochemical DNA sensor exhibited good discrimination ability to one-base and three-base mismatched ssDNA sequences, and the polymerase chain reaction amplification product of salmonella enteritidis gene sequences were further detected with satisfactory results.

1. Introduction

Rapid and sensitive determination of specific target ssDNA sequences associated with either genetic or pathogenic diseases has aroused great interests, which can be used not only in molecular diagnostics [1–3], but also in pharmaceutical and forensic applications [4,5]. Due to the higher sensitivity and lower detection limit, electrochemical DNA sensor has been widely reported for the detection of target ssDNA sequences from different kinds of samples. Electrochemical analysis is a sensitive detection method with wider linear range and lower detection limit, which can be used for the detection of various kinds of electroactive samples [6–8]. Electrochemical detection of DNA hybridization is commonly based on the measurement of the changes of electrochemical response after the hybridization reaction took place on the surface of working electrode [9]. Therefore the design and preparation of probe ssDNA sequence modified electrode are of great importance in developing the electrochemical DNA sensors [10,11]. Various kinds of transducer surfaces have been devised for the fixation of probe ssDNA sequence, which can result in the high immobilization amounts of ssDNA concentration on the electrode surface with suitable orientation. Hvastkovs et al. [12] and Mao et al. [13] reviewed the developments in electrochemical DNA sensors. In recent years nanoparticle based electrodes have been devised for the immobilization of ssDNA sequence, which exhibit the advantages such as larger surface area and better biocompatibility with increased conductivity [14].

In recent years graphene (GR) has attracted intense research interests due to its specific characteristics including extremely high thermal conductivity, good mechanical strength, fast mobility of charge carriers, large specific surface area and upstanding electrical properties [15–17]. Various methods have been reported for the synthesis of GR, including micromechanical cleavage, chemical vapor deposition, solvothermal synthesis and chemical synthesis [18–20]. Electrochemical methods have also been reported for the efficient synthesis of GR, which exhibit the advantages such as green, fast and easy to control without the contamination of the reduced material [21,22]. Due to its excellent electrocatalytic activity and high adsorption ability, GR is an ideal modifier for the construction of electrochemical sensors [23–25]. For example, Lim et al. applied the epitaxial GR as an anode material for the simultaneous detection of all four DNA bases in double stranded DNA (dsDNA) without a prehydrolysis step [26]. Li et al. applied GR modified electrode towards the electrocatalytic oxidation of dopamine and methanol [27]. Our group also fabricated various GR composite modified electrodes for the electrochemical applications [28,29]. Because GR can provide a favorable microenvironment with large surface area and excellent electronic conductivity, GR based electrode has been used in the electrochemical DNA sensors. Du et al. constructed an electrochemical DNA sensor based on a gold nanoparticle/GR composite film [30]. Bo et al.

* Corresponding authors.
E-mail addresses: swyy26@hotmail.com (W. Sun), lgjqust@126.com (G. Li).

http://dx.doi.org/10.1016/j.msec.2014.12.071
0928-4931/

developed an electrochemical DNA sensor based on GR and polyaniline nanowires modified glassy carbon electrode [31]. Sun et al. applied an electrochemical reduced GR modified electrode for the voltammetric detection of transgenic maize MON810 sequence [32].

Among the nanomaterials used for electrochemical DNA sensors, nanosized metal oxides are suitable matrixes for the immobilization of ssDNA sequence, which exhibit the characteristics including wide electrochemical working window, good biocompatibility, large surface area, high electrical conductivity, chemical and photochemical stability, ease of preparation and excellent substrate adhesion. Due to unique properties of nanostructured nickel oxide (NiO), they can be used for immobilization of different molecules and biomolecules to fabricate sensors and biosensors [33,34]. Also NiO has strong affinity with phosphonates and 5′-terminal phosphate group of ssDNA, which can be used for the immobilization of ssDNA probe in DNA sensors. Noorbakash et al. developed an electrochemical DNA sensor based on the immobilization of ssDNA probe on NiO modified GCE [35]. Mohan et al. applied a nanostructured NiO modified indium tin oxide electrode based electrochemical DNA sensor for the detection of visceral leishmaniasis [36]. However, there are no reports about the application of NiO/GR composite for the preparation of DNA sensor to our best knowledge.

In this paper, a NiO and GR nanocomposite was prepared by electrodeposition directly on the surface of carbon ionic liquid electrode (CILE). Due to the specific electrochemical properties of ionic liquid (IL), CILE has been proven to exhibit many advantages including wider electrochemical windows, better antifouling ability and higher detection sensitivity [37,38]. Therefore CILE has been used as the working electrode in electroanalysis and electrochemical sensors [39,40]. Based on the strong affinity of NiO with the 5′-phosphate group of probe ssDNA sequence, a novel electrochemical DNA sensor was fabricated and used for the detection of target ssDNA sequence with methylene blue (MB) as the indicator. This new electrochemical DNA biosensor was successfully applied to the detection of specific ssDNA sequence of salmonella enteritidis with a dynamic range from 1.0×10^{-13} to 1.0×10^{-6} mol L^{-1}. The polymerase chain reaction (PCR) amplification products of salmonella enteritidis gene were further detected with satisfactory results.

2. Experimental

2.1. Apparatus and reagents

A CHI 750B electrochemical workstation (Shanghai Chenhua Instrument, China) was used to carry out all the electrochemical experiments including electrochemical impedance spectroscopy (EIS), cyclic voltammetry and differential pulse voltammetry. A conventional three-electrode system was composed of a saturated calomel electrode (SCE) as reference electrode, a platinum wire as auxiliary electrode and a modified CILE as working electrode. Scanning electron microscopy (SEM) was obtained by a JSM-7100F scanning electron microscope (Japan Electron Company, Japan).

1-Hexylpyridinium hexafluorophosphate ($HPPF_6$, >99%, Lanzhou Greenchem. ILS. LICP. CAS., China), graphite powder (Shanghai Colloid Chemical Plant, particle size of 30 μm), graphene oxide (GO, Taiyuan Tanmei Co., China), $Ni(NO_3)_2 \cdot 6H_2O$ (Tianjin Kwong Shing Ltd. Co., China) and methylene blue (MB, Shanghai Chemical Plant, China) were used as received. Different kinds of buffers such as 0.2 mol L^{-1} PBS (pH 8.0), 50.0 mmol L^{-1} PBS (pH 7.0), acetate buffer solution (pH 4.0), 50.0 mmol L^{-1} Tris–HCl buffer solution (pH 7.0) and 1 × TAE buffer (40.0 mmol L^{-1} Tris + 1.0 mmol L^{-1} EDTA + 40.0 mmol L^{-1} acetate, pH 8.0) were used in the experiment. All the solutions were prepared with doubly distilled water and other chemicals used were of analytical reagents grade.

24-Base sequences, which were selected from salmonella enteritidis gene sequence, were purchased from Shanghai Sangon Biological Engineering Tech. Ltd. Co. (China) with the following sequences.

Probe ssDNA: 5′-TGC AGC GAG CAT GTT CTG GAA AGC-3′;

Target ssDNA: 5′-GCT TTC CAG AAC ATG CTC GCT GCA-3′;

One-base mismatched ssDNA: 5′-GCT TTC CAG AAC ACG CTC GCT GCA-3′;

Three-base mismatched ssDNA: 5′-ACT TTC CAG AAC ACG CTC GCT GTA-3′;

Non-complementary ssDNA: 5′-TTC GCT ACC CGT GCT GAT CTA CGC-3′.

The DNA sample for polymerase chain reaction (PCR) amplification was extracted from salmonella enteritidis gene. The PCR reaction was performed on an Eppendorf Mastercycler Gradient PCR system (Eppendorf, Germany) using oligonucleotide primers for salmonella enteritidis gene with the following sequences:

Primer F: 5′-TTG ATG TGG TTG GTT CGT CAC T-3′;

Primer R: 5′-TCC CTG AAT CTG AGA AAG AAA AAC TC-3′.

2.2. Fabrication of the modified electrode

CILE was fabricated based on the reported procedure [41]. In brief 1.6 g of graphite powder and 0.8 g of $HPPF_6$ was mixed thoroughly in a mortar to get the IL modified carbon paste, which was inserted into a glass tube ($\Phi = 4$ mm) tightly. A copper wire was inserted to one end to establish an electrical contact and the surface of CILE was smoothed on a piece of weighing paper just before use. The newly prepared CILE was inserted into a 1.0 mg ml^{-1} GO solution and electroreduction was performed at the potential of −1.3 V for 600 s to get the electroreduced GR modified CILE [42]. According to the procedure reported in reference [43], NiO nanoparticles were further electrodeposited onto the newly prepared GR/CILE with multi-sweep cyclic voltammetric method in the potential range from 0.5 V to −1.0 V for 20 scans at a scan rate of 70 mV s^{-1} in acetate buffer solution (pH 4.0) containing 1.0 mmol L^{-1} nickel nitrate. The potential was repetitively cycled (30 scans) from −1.0 V to 1.5 V at a scan rate of 100 mV s^{-1} in fresh phosphate solution for the electrodissolution and passivation of a nickel oxide layer on GR/CILE. The resulted electrode was denoted as NiO/GR/CILE and used as the substrate electrode for the further modification.

2.3. Preparation of electrochemical DNA sensor

By using NiO/GR/CILE as the basal electrode, electrochemical DNA sensor was fabricated with the following procedure. Firstly a 10.0 μL of 1.0×10^{-6} mol L^{-1} probe ssDNA solution (in 50.0 mmol L^{-1} pH 7.0 PBS) was directly dropped onto the surface of NiO/GR/CILE. Due to the presence of phosphate group in the 5′ end of the ssDNA probe, nano-NiO can adsorb ssDNA sequence due to its strong affinity to the phosphate group. Then the electrode was washed with 0.5% sodium dodecyl sulfate (SDS) solution and doubly distilled water for 3 times successively to remove unadsorbed probe ssDNA sequence on the surface. This probe ssDNA captured modified electrode was denoted as ssDNA/NiO/GR/CILE.

2.4. Hybridization

The efficient drop hybridization procedure was further used for the target ssDNA sequence hybridized with the probe ssDNA sequence modified electrode [45,46], which was performed by dropping 8.0 μL of target ssDNA sequence (in 50.0 mmol L^{-1} PBS) directly on to the surface of ssDNA/NiO/GR/CILE. The hybridization between the target ssDNA sequence and the probe ssDNA sequence was allowed to proceed for 30 min at room temperature. Then the electrode was washed with 0.5% SDS solution and doubly distilled water for 3 times to remove the unhybridized target ssDNA sequence. This hybridized electrode was further named as dsDNA/NiO/GR/CILE.

2.5. Electrochemical detection

The hybridized electrode was immersed into a 2.0×10^{-5} mol L^{-1} MB MB solution for 10 min to accumulate MB molecules on the electrode surface and then it was washed by 50.0 mmol L^{-1} PBS for 3 times. Electrochemical measurement was performed in a 50.0 mmol L^{-1} Tris–HCl buffer solution (pH 7.0) and the electrochemical response of MB was recorded by differential pulse voltammetric method with the experimental parameters set as: pulse amplitude 0.008 V, pulse width 0.05 s and pulse period 0.2 s.

2.6. PCR amplification of salmonella enteritidis gene

The samples containing salmonella enteritidis were obtained from the rotten eggs, which were minced into tiny pieces, placed in 10 mL concentrated digestion solution and incubated for 48 h in water bath at 25 °C. Then the sample solution was centrifuged at 12000 rpm for 4 min to obtain the precipitate, which was redispersed in 100 μL sterilized distilled water. Then the DNA sequence was extracted from the sample solution by using a DNA extraction kit (Beijing Tiangen Biotech. Ltd. Co., China) with the recommended procedure.

The amplification of salmonella enteritidis gene fragments was performed in a final volume of 25 μL containing 200.0 nmol L^{-1} each primer of salmonella enteritidis gene sequence (primer F and primer R), 10× reaction buffer B (Promega, USA), 2.0 mmol L^{-1} $MgCl_2$, 200.0 nmol L^{-1} each of dATP, dCTP, dGTP and dTTP, 1.5 units of Taq DNA polymerase (Promega, USA), and 1.0 μL DNA template sequence extracted from samples. During the PCR procedure, DNA was initially denatured at 94 °C for 30 s, and PCR experiment was performed for 35 cycles of amplification (94 °C for 30 s, 56 °C for 30 s, 72 °C for 30 s) and final extension at 72 °C for 5 min. Then 6 μL of the PCR products were analyzed by electrophoresis separation at 5 V cm^{-1} for 40 min on a 2% agarose gel, which contained 0.5 μg mL^{-1} of ethidium bromide in 1 × TAE buffer (pH 8.0). Finally the PCR products of salmonella enteritidis gene were kept at 4 °C before use.

After the PCR amplification the product was diluted with 20.0 mmol L^{-1} PBS (pH 7.0), and heated in a boiling water bath for 10 min with the further cooling in an ice water bath for 2 min. By this procedure the resulted dsDNA was denatured to ssDNA and further used for the electrochemical detection by the proposed procedure.

3. Results and discussion

3.1. SEM images of the nanomaterials on the electrode surface

Fig. 1 showed the SEM images of different nanomaterials on the electrode surface. After electrodeposition of GO on CILE, the typical lamellar structure of GR could be observed on the electrode interface (Fig. 1A), which was highly beneficial in maintaining a large effective electrode surface. Electrochemical reduction of GO has been proven to be a facial and controllable method to synthesize GR nanosheets directly on the electrode surface [42]. By controlling the electrodeposition conditions, the oxygenal groups on the GO nanosheets can be reduced with the recovery of the GR nanosheets. After the electrodeposition of NiO nanoparticles, it can be seen that many small particles with the average diameters of 125 nm appeared on the electrode surface, which indicated the successful formation of nanosized NiO. Electrodeposition is a simple and effective method for the preparation of NiO nanoparticles directly on the electrode, which has been reported in the fabrication of the modified electrodes [35,36,43]. Therefore NiO nanoparticles and GR nanosheets were successfully formed on the electrode surface by electrodeposition.

3.2. Electrochemical characterization of the modified electrodes

Cyclic voltammetry has been widely used as an effective method to measure the current change of the modified electrodes. As shown in Fig. 2A, cyclic voltammograms of different modified electrodes in a $[Fe(CN)_6]^{3-/4-}$ solution were recorded and displayed. On bare CILE the redox peak currents were the smallest (curve a). When GR was electrodeposited onto CILE surface, the redox peak currents turned to be the maximum (curve c), which was ascribed to the presence of GR on the electrode. GR has large specific surface area, small band gap, excellent electrical conductivity and high electron transfer capacity. So the electrochemical responses were greatly increased on GR/CILE. After nano-NiO was further modified on the GR/CILE surface, the redox peak currents decreased (curve b), which could be due to the presence of semiconductive NiO nanoparticles on the electrode surface that slowed down the electron transfer of $[Fe(CN)_6]^{3-/4-}$. The changes of the redox peak currents proved the successful deposition of nanocomposite on the electrode surface.

EIS is further used to explore the interfacial information after the modification on the electrode, which is commonly used for the evaluation of the electrochemical information such as electrolyte resistance, electron transfer resistance (Ret) and faradaic capacitance of a given system. The diameter of the semicircle usually equals to the Ret, which controls the electron transfer kinetics of the redox probe at the electrode interface [44]. The EIS experiments were perform in a 10.0 mmol L^{-1} $[Fe(CN)_6]^{3-/4-}$ and 0.1 mol L^{-1} KCl solution with the frequency swept from 10^4 to 1.0 Hz and the results were shown in Fig. 2B. On CILE the Ret value was gotten as 196.3 Ω (curve a) and that of GR/CILE was close to zero with a straight line appeared (curve c), which indicated the formation of high conductive GR on the electrode. With the further deposition of NiO on GR/CILE surface, the Ret value increased to 75.1 Ω (curve b), which could be attributed to the formation of semiconductive NiO nanoparticles on the electrode that further

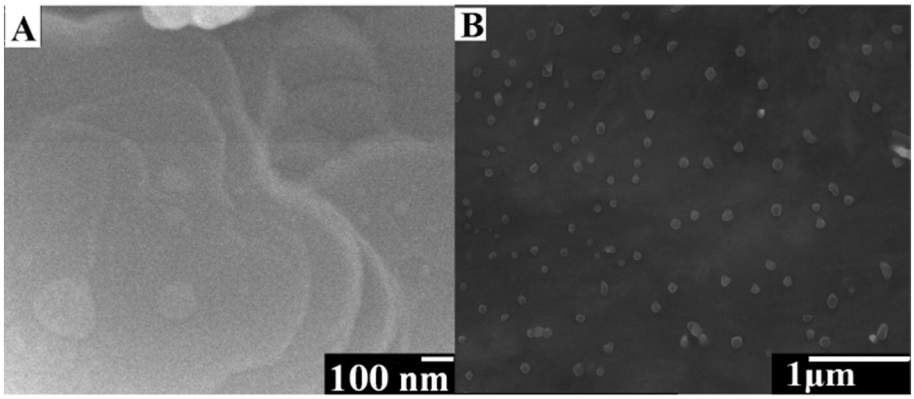

Fig. 1. SEM images of GR/CILE (A) and NiO/GR/CILE (B).

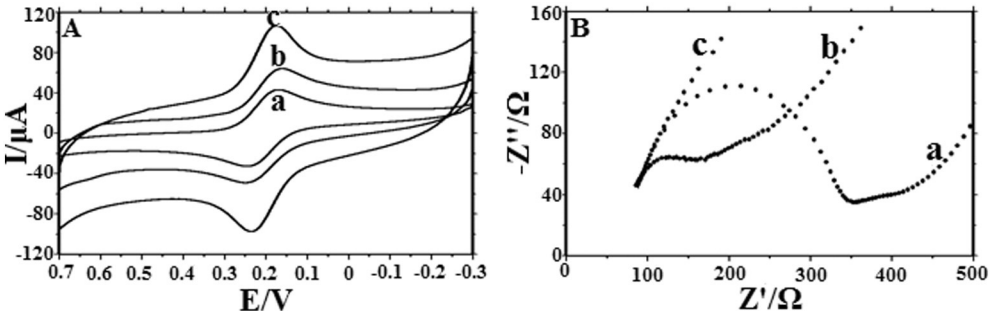

Fig. 2. (A) Cyclic voltammograms of (a) CILE, (b) NiO/GR/CILE and (c) GR/CILE in a 1.0 mmol L^{-1} $[Fe(CN)_6]^{3-/4-}$ and 0.5 mol L^{-1} KCl solution with the scan rate of 100 mV s^{-1}. (B) EIS of (a) CILE, (b) NiO/GR/CILE and (c) GR/CILE in a 10.0 mmol L^{-1} $[Fe(CN)_6]^{3-/4-}$ and 0.1 mol L^{-1} KCl solution.

hinder the electron transfer. The EIS results were in good accordance with CV data, indicating the successful preparation of the nanocomposite modified electrode.

3.3. Electrochemical behaviors of MB on different modified electrodes

Differential pulse voltammetric responses of MB on different ssDNA modified electrodes were recorded in a 50.0 mmol L^{-1} Tris–HCl (pH 7.0) solution with the results shown in Fig. 3. On ssDNA/CILE (curve a) MB exhibited a well-defined reduction peak at −0.28 V, which was due to the electrochemical reduction of phenothiazine group in MB structure. MB can interact with the guanine base of ssDNA sequence and be accumulated on the electrode surface, so the electrochemical response of Mb can be observed. On ssDNA/GR/CILE (curve b) the reduction peak current increased greatly, indicating that the presence of GR with large surface area on the electrode increased the adsorption amounts of ssDNA sequence. Also the high conductive GR is beneficial for the electrochemical reaction of MB. On ssDNA/NiO/CILE (curve c) the electrochemical response also increased greatly, which could be attributed to the specific affinity of NiO with 5′-phosphate group on ssDNA sequence that could adsorb more ssDNA sequence, and the further accumulation of MB molecules on the electrode surface. On ssDNA/NiO/GR/CILE (curve d) the biggest reduction peak of MB appeared, which could be attributed to the synergistic effects of NiO nanoparticles and GR on the electrode surface. The presence of GR nanosheets on CILE surface increases the effective surface area with more NiO nanoparticles deposited on its surface, which adsorbs more ssDNA sequence on the electrode surface, and then more guanines are exposed and can further accumulate more MB molecules by the interaction. Also the high conductivity of GR on the electrode is helpful to increase the electron transfer rate of MB with electrode, so the biggest response of MB could be achieved on ssDNA/NiO/GR/CILE.

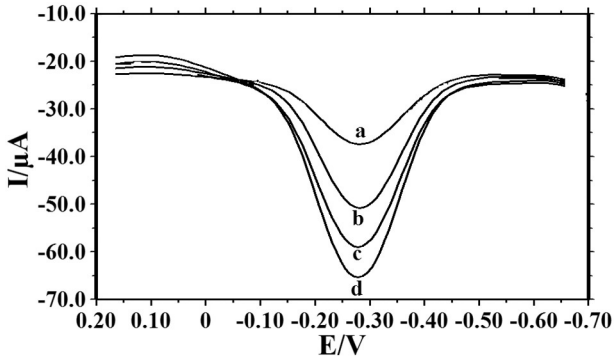

Fig. 3. Differential pulse voltammograms of (a) ssDNA/CILE, (b) ssDNA/GR/CILE, (c) ssDNA/NiO/CILE and (d) ssDNA/NiO/GR/CILE in a 50.0 mmol L^{-1} pH 7.0 Tris–HCl buffer containing 2.0×10^{-5} mol L^{-1} MB.

3.4. Selectivity of the electrochemical DNA biosensor

MB is a kind of phenothiazine dye that is commonly used as the electrochemical indicator in DNA biosensor [47], which can interact with ssDNA or dsDNA by different interaction models and result in the changes of the electrochemical response. MB can interact with negative charged phosphate framework of ssDNA by electrostatic binding, or intercalate into the major or minor helix grooves of dsDNA structure, or bind between MB and guanine base [48]. The binding model often changes and depends on the experimental conditions used for the interaction [49]. The selectivity of this electrochemical DNA biosensor to different mismatched ssDNA sequences was investigated by using probe ssDNA/NiO/GR/CILE to hybridize with 1.0×10^{-6} mol L^{-1} different ssDNA sequences and the results were shown in Fig. 4. The biggest reduction peak of MB appeared on ssDNA/NiO/GR/CILE (curve a), which was attributed to the electrochemical reaction of MB that interacted with the guanine bases of ssDNA on the electrode surface. After hybridized with complementary ssDNA sequence, the electrochemical response decreased greatly with the smallest reduction peak current appeared (curve e). The result indicated the successful hybridization of probe ssDNA sequence with target ssDNA sequence to form a dsDNA structure on the electrode surface. Because ssDNA sequence was adsorbed on the surface of NiO/GR/CILE, MB could interact with the guanine groups of ssDNA and accumulate on the electrode surface. After hybridization dsDNA was formed on the electrode interface with guanine groups wrapped up in the duplex structure, so the specific interaction of MB with guanine residues was prevented after hybrid formed on the surface. Therefore the smallest electrochemical response

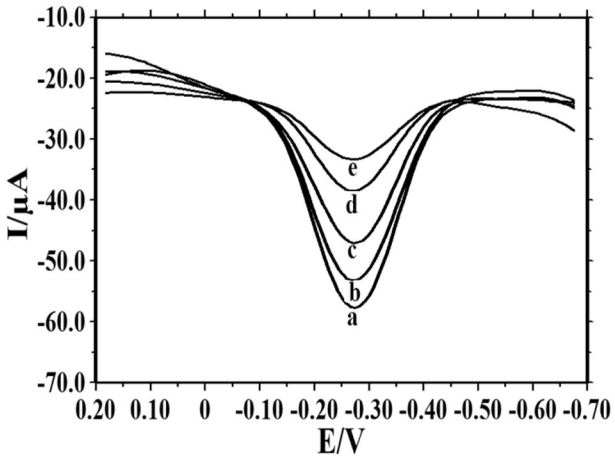

Fig. 4. Differential pulse voltammograms of 2.0×10^{-5} mol L^{-1} MB at ssDNA/NiO/GR/CILE (a) and after hybridization with 1.0×10^{-6} mol L^{-1} of noncomplementary ssDNA sequence (b), three-base mismatched ssDNA sequence (c), one-base mismatched ssDNA sequence (d) and complementary ssDNA sequence (e).

appeared. After hybridization with the noncomplementary ssDNA sequence (curve b), the electrochemical response of MB was a little smaller than that of the probe ssDNA modified electrode (curve a), which indicated that some noncomplementary ssDNA sequence may be adsorbed on the electrode surface and blocked the guanine residues of the probe ssDNA sequence. After ssDNA/NiO/GR/CILE was hybridized with three-base mismatched sequence (curve c) and one-base mismatched sequence (curve d), the reduction peak currents decrease in turn. The results indicated that the partially formation of dsDNA duplex structure with the mismatched sequence took place on the electrode and the amount of guanine residues exposed to MB was decreased gradually, then the electrochemical response decreased. It is worth to note that the reduction peak current of three-base mismatched ssDNA sequence was obviously higher than that of one-base mismatched ssDNA sequence, which demonstrated that this DNA biosensor exhibited high selectivity and good distinguish ability for the hybridization detection.

3.5. Sensitivity of the electrochemical DNA biosensor

The sensitivity of this electrochemical DNA sensor was investigated by using the probe ssDNA modified electrode to hybridize with different concentrations of the complementary target ssDNA sequence. As shown in Fig. 5, the reduction current of MB decreased with the concentration of complementary target ssDNA sequence in the range from 1.0×10^{-13} to 1.0×10^{-6} mol L^{-1} and then tended to remain constant, indicating all the available probe ssDNA sequence on the electrode surface had been involved in the hybridization reaction. Due to the formation of duplex of hybrid dsDNA on the electrode, the interaction of guanine residues with MB was prevented with less MB molecules adsorbed on the electrode, so the electrochemical signals of MB were decreased correspondingly. When the concentration was lower than 1.0×10^{-13} mol L^{-1}, the reduction peak current of MB was almost the same as that without hybridization. The relationship of the reduction peak currents of MB before and after hybridization with logarithmic value of target ssDNA sequence could be plotted with the linear regression equation as $\Delta I(\mu A) = 4.11 \log[c/(\text{mol L}^{-1})] + 58.02$ ($n = 8$, $\gamma = 0.998$), where ΔI is the change of reduction peak current before and after the hybridization reaction, and c is the concentration of the target ssDNA sequences. The detection limit was calculated as 3.12×10^{-14} mol L^{-1}, which was deduced from $3\ S_0/S$, here 3 is the factor at the 99% confidential level, S_0 is the standard deviation of the blank solution measurements and S is the slope of the calibration curve. This detection limit was lower than the previous reported values such as Fe_3O_4 microsphere-GR composite modified CILE (3.59×10^{-13} mol L^{-1}) [50], multi-walled carbon nanotubes and gold nanoparticles modified gold electrode (7.5×10^{-12} mol L^{-1}) [51], gold nanoparticle and GR modified electrode (2.9×10^{-13} mol L^{-1}) [52].

The relative standard deviation (RSD) of the reduction peak current for the six repeated detections of 1.0×10^{-7} mol L^{-1} target ssDNA sequence was calculated as 3.7%, indicating the good reproducibility of this method. The stability of ssDNA/NiO/GR/CILE was investigated after 10 day storage at 4 °C and further used to hybridize with the target ssDNA sequence, 96.3% of the initial sensitivity remained, indicating that this modified electrode was a stable platform as electrochemical DNA biosensor.

3.6. Detection of PCR products of salmonella enteritidis gene sequence

The PCR products of salmonella enteritidis gene sequence were denatured by heating the solution in a boiling water bath for 10 min and then frozen in an ice water bath for 2 min to obtain the sample solution containing ssDNA sequence. By dropping 6.0 μL of ssDNA sample solution on the surface of ssDNA/NiO/GR/CILE with the following hybridization and electrochemical detection performed under the experimental procedures, differential pulse voltammetric curves were recorded and shown in Fig. 6. On ssDNA/NiO/GR/CILE the biggest electrochemical response of MB appeared (curve a), which was due to the interaction of MB with guanine groups of ssDNA sequence on the electrode. After hybridization with the sample solution the electrochemical signal of MB decreased (curve b), which indicated the successful formation of dsDNA structure on the electrode, the guanine groups were wrapped inside the duplex structure of dsDNA and could not interact with MB. This significant difference of the MB signals between ssDNA/NiO/GR/CILE (curve a) and the hybridized electrode (curve b) proved that this electrochemical DNA biosensor could effectively detect the PCR product of salmonella enteritidis gene sample. While the smallest responses appeared at NiO/GR/CILE (curve c), indicating that the presence of ssDNA sequence on the electrode surface played important roles in the accumulation of MB on the electrode.

4. Conclusions

By using electrochemical reduction method GR nanosheets and NiO nanoparticles were deposited on the surface of CILE step-by-step to get a NiO/GR/CILE, which was further used for the immobilization of probe ssDNA sequence. The presence of GR and NiO nanocomposite gives a biocompatible platform with large surface area and the strong ability to bind the phosphate groups of probe ssDNA sequence. After hybridization with the target salmonella enteritidis ssDNA sequence, the decrease of the reduction peak current of MB was proportional to the

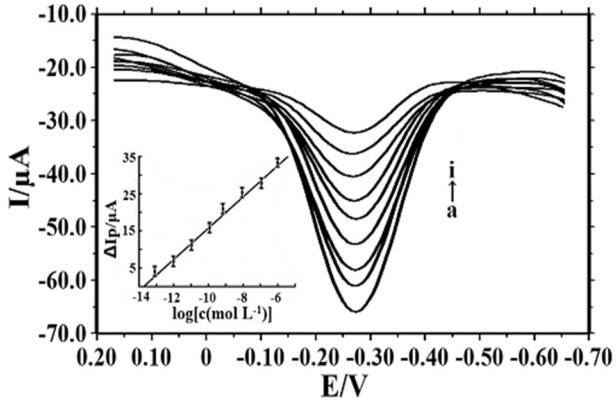

Fig. 5. Differential pulse voltammograms of MB on ssDNA/NiO/GR/CILE after hybridization with different concentrations of target ssDNA sequence (from a to i were 0, 1.0×10^{-13} mol L^{-1}, 1.0×10^{-12} mol L^{-1}, 1.0×10^{-11} mol L^{-1}, 1.0×10^{-10} mol L^{-1}, 1.0×10^{-9} mol L^{-1}, 1.0×10^{-8} mol L^{-1}, 1.0×10^{-7} mol L^{-1} and 1.0×10^{-6} mol L^{-1}, respectively). Inset: plots of the changes of the reduction peak current before and after hybridization versus logarithm of target ssDNA concentration.

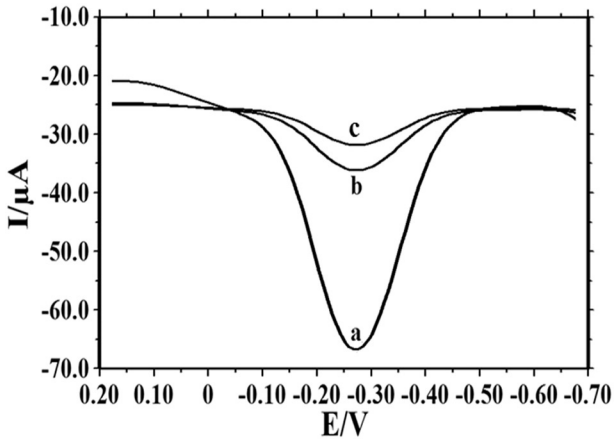

Fig. 6. Differential pulse voltammograms of MB at ssDNA/NiO/GR/CILE (a), hybridized with PCR product of salmonella enteritidis (b) and NiO/GR/CILE (c).

concentration of target ssDNA sequence in the range from 1.0×10^{-13} to 1.0×10^{-6} mol L^{-1} with a detection limit of 3.12×10^{-14} mol L^{-1} (3σ). The electrochemical DNA sensor showed excellent discrimination ability to the detection of different ssDNA sequence and was further applied to the PCR product of salmonella enteritidis gene with satisfactory results.

Acknowledgments

We acknowledge the financial support of the National Natural Science Foundation of China (No. 21365010, 51363008), the Natural Science Foundation of Shandong Province (ZR2013BM014), the Nature Science Foundation of Hainan Province (213015, 214022) and the Project of Hainan Applied Technology Research and Development (ZDXM2014098).

References

[1] F.R.R. Teles, L.P. Fonseca, Talanta 77 (2008) 606–623.
[2] A. Bonanni, M. del Valle, Anal. Chim. Acta 678 (2010) 7–17.
[3] M.I. Pividori, A. Merko, S. Alegret, Biosens. Bioelectron. 15 (2000) 291–303.
[4] E. Mateo-Martí, C. Briones, C.M. Pradier, J.A. Martín-Gago, Biosens. Bioelectron. 22 (2007) 1926–1932.
[5] S.A. Soper, K. Brown, A. Ellington, B. Frazier, G. Garcia-Manero, V. Gau, Biosens. Bioelectron. 21 (2006) 1932–1942.
[6] M. Bojdi, M. Behbahani, A. Sahragard, B.G. Amin, A. Fakhari, A. Bagheri, Electrochim. Acta 149 (2014) 108–116.
[7] H. Hosseini, M. Behbahani, M. Mahyari, H. Kazerooni, A. Bagheri, A. Shaabani, Biosens. Bioelectron. 59 (2014) 412–417.
[8] M. Bojdi, M. Hossein, M. Zadeh, M. Behbahani, A. Farahani, Electrochim. Acta 136 (2014) 59–65.
[9] J.P. Tosar, G. Branas, J. Laiz, Biosens. Bioelectron. 26 (2010) 1205–1217.
[10] J. Wang, Anal. Chim. Acta 500 (2003) 247–257.
[11] G.J. Li, L.H. Liu, X.W. Qi, W. Sun, X.L. Li, Electrochim. Acta 63 (2012) 312–317.
[12] E.G. Hvastkovs, D.A. Buttry, Analyst 135 (2010) 1817–1829.
[13] X. Mao, G.D. Liu, J. Biomed. Nanotechnol. 4 (2008) 419–431.
[14] K. Xu, J.R. Huang, Z.Z. Ye, Y.B. Ying, Y.B. Li, Sensors 9 (2009) 5534–5557.
[15] A.K. Geim, K.S. Novoselov, Nat. Mater. 6 (2007) 183–191.
[16] D. Li, M.B. Müller, S. Gilje, R.B. Kaner, G.G. Wallace, Nat. Nanotechnol. 3 (2008) 101–105.
[17] D. Chen, L. Tang, J. Li, Chem. Soc. Rev. 39 (2010) 3157–3180.
[18] X. Huang, X.Y. Qi, F. Boey, H. Zhang, Chem. Soc. Rev. 41 (2012) 666–686.
[19] H.J. Jiang, Small 7 (2011) 2413–2427.
[20] S. Park, R.S. Ruoff, Nat. Nanotechnol. 4 (2009) 217–224.
[21] H.L. Guo, X.F. Wang, Q.Y. Qian, F.B. Wang, X.H. Xia, ACS Nano. 3 (2009) 2653–2659.
[22] F. Gao, X.W. Qi, X.L. Cai, Q.X. Wang, F. Gao, W. Sun, Thin Solid Films 520 (2012) 5064–5069.
[23] Y.Y. Shao, J. Wang, H. Wu, J. Liu, I.A. Aksay, Y.H. Lin, Electroanalysis 22 (2010) 1027.
[24] D.A.C. Brownson, D.K. Kampouris, E. Banks, Chem. Soc. Rev. 41 (2012) 6944–6976.
[25] M. Pumera, A. Ambrosi, A. Bonanni, E.L.K. Chng, H.L. Poh, Trends Anal. Chem. 29 (2010) 954–965.
[26] C.X. Lim, H.Y. Hoh, P.K. Ang, K.P. Loh, Anal. Chem. 82 (2010) 7387–7393.
[27] Y. Li, L. Tang, J. Li, Electrochem. Commun. 11 (2009) 846–849.
[28] W. Sun, X.Z. Wang, H.H. Zhu, X.H. Sun, F. Shi, G.N. Li, Z.F. Sun, Sens. Actuators B 178 (2013) 443–449.
[29] W. Sun, X.Z. Wang, X.H. Sun, Y. Deng, J. Liu, B.X. Lei, Z.F. Sun, Biosens. Bioelectron. 44 (2013) 146–151.
[30] M. Du, T. Yang, K. Jiao, J. Mater. Chem. 20 (2010) 9253–9260.
[31] Y. Bo, H.Y. Yang, Y. Hu, T.M. Yao, S.S. Huang, Electrochim. Acta 56 (2011) 2676–2681.
[32] W. Sun, Y.X. Lu, Y.J. Wu, Y.Y. Zhang, P. Wang, Y. Chen, G.J. Li, Sensors Actuators B 202 (2014) 160–166.
[33] A. Salimi, E. Sharifi, A. Noorbakhsh, S. Soltanian, Biophys. Chem. 125 (2007) 540–548.
[34] A. Salimi, A. Noorbakhsh, H. Rafiee-Pour, H. Ghourchian, Electroanalysis 23 (2011) 6831–6835.
[35] A. Noorbakash, A. Salimi, Biosens. Bioelectron. 30 (2011) 188–196.
[36] S. Mohan, P. Srivastava, S.N. Maheshwari, S. Sunder, R. Prakach, Analyst 136 (2011) 2845–2851.
[37] M.J.A. Shiddiky, A.A.J. Torriero, Biosens. Bioelectron. 26 (2011) 1775–1787.
[38] M. Opallo, A. Lesniewski, Electrochim. Chem. 656 (2011) 2–16.
[39] W. Sun, P. Qin, H.W. Gao, G.C. Li, K. Jiao, Biosens. Bioelectron. 25 (2010) 1264–1270.
[40] W. Sun, Y.Z. Li, M.X. Yang, J. Li, K. Jiao, Sensors Actuators B 133 (2008) 387–392.
[41] W. Sun, M.X. Yang, K. Jiao, Anal. Bioanal. Chem. 389 (2007) 1283–1291.
[42] M. Zhou, Y.L. Wang, Y.M. Zhai, J.F. Zhai, W. Ren, F. Wang, S.J. Dong, Chem. Eur. J. 15 (2009) 6116–6120.
[43] D. Giovanelli, N.S. Lawrence, S.J. Wilkins, L. Jiang, T.G.L. Jones, R.G. Compton, Sensors Actuators B 88 (2003) 320–328.
[44] M.E. Orazem, B. Tribollet, Electrochemical Impedance Spectroscopy, Wiley-Interscience, 2008.
[45] M.S. Hejazi, M.H. Pournaghi-Azar, E. Alipour, F. Karimi, Biosens. Bioelectron. 23 (2008) 1588–1594.
[46] X.W. Qi, H.W. Gao, Y.Y. Zhang, X.Z. Wang, Y. Chen, W. Sun, Bioelectrochemistry 88 (2012) 42–47.
[47] D. Pan, X.L. Zuo, Y. Wan, L.H. Wang, J. Zhang, S.P. Song, C.H. Fan, Sensors 7 (2007) 2671–2680.
[48] H. Nasef, V. Beni, C.K. O'Sullivan, Anal. Bioanal. Chem. 396 (2010) 1423–1432.
[49] P. Kara, K. Kerman, D. Ozkan, B. Meric, A. Erdem, Z. Ozkan, M. Ozsoz, Electrochem. Commun. 4 (2002) 705–709.
[50] W. Sun, X.W. Qi, Y. Chen, S.Y. Liu, H.W. Gao, Talanta 87 (2011) 106–112.
[51] H.Y. Ma, L.P. Zhang, Y. Pan, K.Y. Zhang, Y.Z. Zhang, Electroanalysis 20 (2008) 1220–1226.
[52] W. Sun, X.W. Qi, Y.Y. Zhang, H.R. Yang, H.W. Gao, Y. Chen, Z.F. Sun, Electrochim. Acta 85 (2012) 145–151.